

THE CRYSTAL STRUCTURES OF THE HUMITE MINERALS: I. NORBERGITE

G. V. GIBBS AND P. H. RIBBE, *Department of Geological Sciences, Virginia Polytechnic Institute, Blacksburg, Virginia 24061.*

ABSTRACT

The crystal structure of norbergite, $\text{Mg}_2\text{SiO}_4 \cdot \text{MgF}_{1.8}(\text{OH})_{0.2}$ from Franklin, New Jersey ($a=4.7104(1)$; $b=10.2718(3)$; $c=8.7476(4)$ Å; $P6mm$, $\rho_{(0^{\circ})2\theta}=3.177$ g/cc) was refined by least-squares techniques to $R=0.052$ using 867 intensities weighted by the range-estimate method (weighted $R=0.024$). The structure is based on a slightly distorted hexagonal close-packed array of anions with one-half the octahedral sites occupied by Mg and one-twelfth the tetrahedral sites occupied by Si. F is ordered in the array and bonded to three Mg; its temperature factor is twice that of four-coordinated O. Comparable bond lengths involving F and O indicate that the radius of F is ~ 0.11 Å smaller than that of O.

As in forsterite, the dominant structural unit in norbergite is a zigzag chain of edge-sharing octahedra lying parallel to z . A detailed study of the structure in terms of bond-angle strains shows that the distortions from an ideal hexagonal close-packed model can be explained qualitatively in terms of cation-cation repulsion across shared polyhedral edges. The Si-O bond lengths (1.635, 1.638 Å) opposite shared edges are significantly longer than that (1.612 Å) opposite the unshared edges of the tetrahedron.

INTRODUCTION

In 1894 Penfield and Howe recognized that the humite minerals are morphotropic with the general formula $n\text{Mg}_2\text{SiO}_4\text{Mg}(\text{F},\text{OH})_2$, where $n=4$ for clinohumite, $n=3$ for humite and $n=2$ for chondrodite. They predicted the existence of norbergite ($n=1$) which was later discovered by Geijer (1926). The a and b cell parameters of all the humites were found to be very similar to those of forsterite and on this basis Bragg and West (1927) and Taylor and West (1928, 1929) proposed structures for the humites which are based on a hexagonal close-packed array of anions similar to that of forsterite (described by Bragg and Brown, 1926). Taylor and West (1928, 1929) assumed from charge-balance considerations that the (F,OH) anions are bonded to three Mg, whereas the oxygen anions, as in forsterite, are bonded to one tetrahedrally-coordinated Si and three octahedrally-coordinated Mg cations. This requires ordering of the (F, OH) anions within the structure. They described the structures in terms of "unit blocks" of $\text{Mg}(\text{F},\text{OH})_2$ and Mg_2SiO_4 composition. Ribbe, Gibbs and Jones (1968) have recently pointed out that although the "unit blocks" in their drawings of the idealized structures are correct (*cf.* Bragg and Claringbull, 1965, Fig. 122), their compositions are in fact $\text{Mg}(\text{F},\text{OH})\text{O}$ and $\text{Mg}_2\text{SiO}_3(\text{F},\text{OH})$.

The present study of the humite minerals has been undertaken as part of a larger study of the inductive effects and spatial distribution of coordinating cations on the Si-O bond in certain nesosilicates (garnets,

olivines, humites). Of further interest are the effects of $F \rightleftharpoons O$ substitutions, the possibility of cation ordering, and the steric details of the polyhedral elements in humites.

A preliminary paper in this series discusses the cation and anion substitutions in the humite minerals and their structural similarities with olivine (Ribbe *et al.*, 1968); a second is concerned with the crystal chemistry of natural humites based on 55 microprobe analyses and precise cell parameter measurements on 8 of these specimens (Jones, Ribbe and Gibbs, 1969). This paper presents the results of a detailed three-dimensional structure analysis of norbergite; subsequent papers will describe structure analyses of chondrodite, humite, clinohumite and titanoclinohumite.

EXPERIMENTAL PROCEDURES

The norbergite specimen used in this study was kindly loaned to us by the Smithsonian Institution; the microprobe analysis, density and refractive indices are listed in Table 1. Weissenberg photographs of zero and higher levels about the *a* and *c* axes were found to

TABLE 1. MICROPROBE ANALYSIS AND PHYSICAL PROPERTIES OF NORBERGITE FROM FRANKLIN, N. J., U. S. NATIONAL MUSEUM SPECIMEN #R 12213

<i>Microprobe analysis</i> (Jones <i>et al.</i> , 1969).			
SiO ₂	29.74 wt. %	CaO	0.15
FeO	0.06	ZnO	0.05
MnO	0.01	F	16.77
MgO	58.73	OH (calc.)	1.44
TiO ₂	0.42	Total, corrected for F, OH:	99.64 wt. %
<i>Density:</i> observed, 3.177 g/cc.; calculated, 3.186 g/cc.			
<i>Chemical formula</i> normalized to one Si.			
$Mg_{1.983}Fe_{0.002}Ca_{0.006}Zn_{0.001}SiO_4 \cdot Mg_{6.983}Ti_{0.011}F_{1.805}OH_{0.173}O_{0.022}$			
<i>Unit cell parameters</i> (Jones <i>et al.</i> , 1969) compared with those for synthetic $Mg_2SiO_4 \cdot MgF_2$ (Van Valkenburg, 1961). Estimated standard errors in brackets refer to the last decimal place.			
	Specimen #R 12213	Synthetic norbergite	
<i>a</i>	4.7104 (1) Å	4.709 Å	
<i>b</i>	10.2718 (3)	10.271	
<i>c</i>	8.7476 (4)	8.727	
<i>V</i>	423.24 Å ³	422.22 Å ³	
<i>Z</i>	4	4	
<i>Refractive indices</i>			
α	1.559		
β	1.564	$2V_{(calc)} = 53.7^\circ$	
γ	1.584		

TABLE 3. POSITIONAL PARAMETERS, ISOTROPIC TEMPERATURE FACTORS, AND R.M.S. EQUIVALENTS FOR NORBERGITE^a

Atom	Site symmetry	<i>x</i>	<i>y</i>	<i>z</i>	<i>B</i> (Å ²)	(μ)(Å)
M(3)	C ₁	0.9890(2)	0.6330(1)	0.4305(1)	0.33(2)	0.065(2)
M(2)	C _s	.9924(2)	.9077(2)	.2500	.38(3)	.069(3)
Si	C _s	.4195(2)	.7196(1)	.2500	.28(2)	.060(2)
O(1)	C _s	.7617(4)	.7204(3)	.2500	.38(5)	.069(5)
O(2)	C _s	.2793(5)	.5740(3)	.2500	.32(5)	.064(5)
O(3)	C ₁	.2690(3)	.7907(2)	.1034(3)	.32(4)	.064(4)
F	C ₁	.7295(3)	.9682(2)	.0834(3)	.74(3)	.097(2)

^a Estimated standard deviations are in brackets and refer to the last decimal place.

exhibit systematic presences and Laue symmetry consistent with space group *Pbnm* determined for norbergite by Taylor and West (1929). Cell edges were measured using a precision back-reflection Weissenberg camera and refined using a least-squares program prepared by Burnham (1962). They are compared in Table 1 with those obtained for synthetic norbergite by Van Valkenburg (1961). Intensity data were recorded for all four quadrants of six levels about *c* with a manually operated Weissenberg single-crystal diffractometer equipped with a scintillation counter. MoK α radiation was used and reasonable monochromatization was accomplished with a Nb filter and pulse height analyzer. The peaks of 867 reflections, traced out on a strip chart and integrated with a planimeter, were corrected for the Lp factors and converted to structural amplitudes. No absorption corrections were applied to the data because the transmission factors are practically constant for MoK α radiation in the range where the data were recorded. Symmetry-equivalent structure amplitudes were averaged to give 293 nonequivalent amplitudes. Estimates of the standard deviations of the averaged structure amplitudes, $\hat{\sigma}(F_0)$, were made using the range estimate as the unbiased estimate of the population standard deviation $\hat{\sigma}(F_0)$ (Ibers, 1956). These data were then submitted to a least-squares refinement (Busing *et al.*, 1962) in which the overall scale factor, s_0 , and the positional and isotropic temperature parameters were varied using weights $w = \hat{\sigma}(F_0)^{-2}$, half-ionized form factors for Mg, Si, O and F taken from the International Tables, Vol. III, and the positional parameters published by Taylor and West. In four cycles the refinement converged, giving an unweighted *R* factor of 0.052 and a weighted *R* of 0.024. The error mean square $(\Sigma w\Delta^2/n-m)^{1/2}$ calculated 1.2 which indicates that the weighting scheme is valid, that the experimental errors are normally distributed and that the estimated standard deviations are reliable and essentially unbiased by systematic error. The observed structure amplitudes, F_0 , the calculated structure factors, s_0F_c , and the estimated standard deviations, $\hat{\sigma}(F_0)$, are listed in Table 2.¹ The final positional and isotropic temperature factors and their estimated standard deviations are given in Table 3. The bond lengths and angles with their estimated standard deviations calculated from the variance-covariance matrix using the program ORFFE (Busing *et al.*, 1964) are listed in Table 4.

¹ Table 2 has been deposited with the National Auxiliary Publication Service. To obtain a copy, order NAPS Document No. 00243 from ASIS National Auxiliary Publications Service, c/o CCM Information Sciences, Inc., 22 West 34th Street, New York, New York 10001; remitting \$1.00 for microfiche or \$3.00 for photocopies, payable to ASIS-NAPS.

TABLE 4. BOND LENGTHS AND BOND ANGLES FOR NORBERGITE^a

Si tetrahedron			M(2) octahedron			
Bond lengths (Ångströms)			Bond lengths (Ångströms)			
Si-O(1)		1.612(2)	M(2)-O(1)			2.209(4)
Si-O(2)		1.635(3)	M(2)-O(2)			2.018(3)
Si-O(3)	[2]	1.638(2)	M(2)-O(3)	[2]		2.188(3)
mean		1.631(1)	M(2)-F	[2]		2.011(2)
			mean			2.104(1)
O(1)-O(2)		2.725(3)	O(1)-O(3) ^b	[2]		2.806(3)
O(1)-O(3)	[2]	2.748(3)	O(2)-O(3)	[2]		3.188(3)
O(2)-O(3) ^a	[2]	2.570(3)	O(3)-O(3) ^a			2.565(5)
O(3)-O(3) ^a		2.565(5)	F-F			2.915(5)
mean		2.654(1)	F-O(1)	[2]		2.936(4)
			F-O(2)	[2]		2.943(3)
			F-O(3)	[2]		3.132(3)
			mean			2.958(1)
Bond angles (degrees)		Strain ^b	Bond angles) degrees)		Strain ^b	
O(1)-Si-O(2)	114.1(1)	+4.6	O(1)-M(2)-O(3)	[2]	79.3(1) -10.7	
O(1)-Si-O(3)	[2]	115.4(1)	+4.9	O(2)-M(2)-O(3)	[2]	98.5(1) + 8.5
O(2)-Si-O(3)	[2]	103.5(1)	-6.0	O(3)-M(2)-O(3)		71.8(1) -18.2
O(3)-Si-O(3)		103.1(1)	-6.4	F-M(2)-F		92.9(1) + 2.9
mean		109.0(1)		F-M(2)-O(1)	[2]	88.0(1) + 2.0
				F-M(2)-O(2)	[2]	93.8(1) + 3.8
				F-M(2)-O(3)	[2]	96.4(1) + 6.4
				mean		88.7(1)
<i>M(3) octahedron</i>						
Bond lengths (Ångströms)						
			M(3)-O(1)		2.108(2)	
			M(3)-O(2)		2.175(2)	
			M(3)-O(3)		2.109(2)	
			M(3)-O(3)1		1.994(3)	
			M(3)-F1		2.038(3)	
			M(3)-F		1.986(2)	
			mean		2.068(1)	
			O(1)-O(2) ^c		2.865(3)	
			O(1)-O(3) ^c		2.806(3)	

(Table 4 continued on following page)

TABLE 4—(continued)

O(1)-O(3)1	3.093(3)	
O(2)-O(3) ^d	2.570(3)	
O(3)-O(3)1	3.085(3)	
F-F1 ^d	2.689(4)	
F-O(1)	2.974(3)	
F-O(2)	3.008(3)	
F1-O(2)	2.957(2)	
F1-O(3)	3.126(3)	
F-O(3)1	2.967(3)	
F1-O(3)1	2.839(3)	
mean	2.915(1)	
Bond angles (degrees)		Strain ^b
O(1)-M(3)-O(2)	84.0(1)	- 6.0
O(1)-M(3)-O(3)	83.4(1)	- 6.6
O(1)-M(3)-O(3)1	97.9(1)	+ 7.9
O(1)-M(3)-F	93.1(1)	+ 3.1
O(2)-M(3)-O(3)	73.7(1)	-16.3
O(2)-M(3)-F	92.5(1)	+ 2.5
O(2)-M(3)-F1	89.1(1)	- 0.9
O(3)-M(3)-O(3)1	97.5(1)	+ 7.5
F-M(3)-F1	83.9(1)	- 6.1
F-M(3)-O(3)1	96.4(1)	+ 6.4
F1-M(3)-O(3)	97.8(1)	+ 7.8
F1-M(3)-O(3)1	89.5(1)	- 0.5
mean	89.9(1)	

^a Estimated standard deviations are in brackets and refer to the last decimal place. Numbers in square brackets are multiplicities.

^b Strain equals the observed angle minus the angle calculated for an ideal hexagonal close-packed structure (cf. Table 5).

^c Edge shared by two octahedra.

^d Edge shared by octahedron and tetrahedron.

An attempt was made to extend the calculation to include a refinement of the anisotropic temperature factors using the results of the isotropic refinement as starting parameters. In two cycles, β_{11} of the O(3) atom calculated nonpositive definite at -0.020 and the unweighted R increased to 0.085 . Two additional cycles resulted in the β_{11} 's of O(2) and O(1) calculating nonpositive definite at 0.004 and 0.002 , respectively, whereas β_{11} of O(3) remained essentially unchanged at -0.021 and R increased further to 0.105 . Examination of the correlation matrix calculated at the end of the fourth cycle revealed a moderate interdependence -0.37 between β_{11} and β_{33} of the O(3) atom; however, it is unlikely that the divergence of the refinement is a manifestation of this interdependence, because more than 85 percent of the variation in β_{11} cannot be explained in terms of a linear dependence on β_{33} and must be due to other factors. It may be that a second order tensor inadequately

describes the thermal vibration of O(3) and that a fourth order tensor is necessary (cf. Waser, 1955). Dr. P. B. Moore (priv. commun.) has suggested that "One of the causes of divergence resulting from anisotropic refinement may be the close parameter correlations inherent in close-packed systems."

DISCUSSION

The structure of norbergite, $Mg_3SiO_4F_2$, is based on a slightly distorted hexagonal close-packed array of anions with one-half the octahedral sites occupied by Mg and one-twelfth the tetrahedral sites occupied by Si. To maintain local charge balance, fluorine is ordered in the close-packed array and bonded to three Mg, whereas O is bonded to three Mg and one Si (as in forsterite—see Birle, Gibbs, Moore and Smith, 1968). Ribbe *et al.*

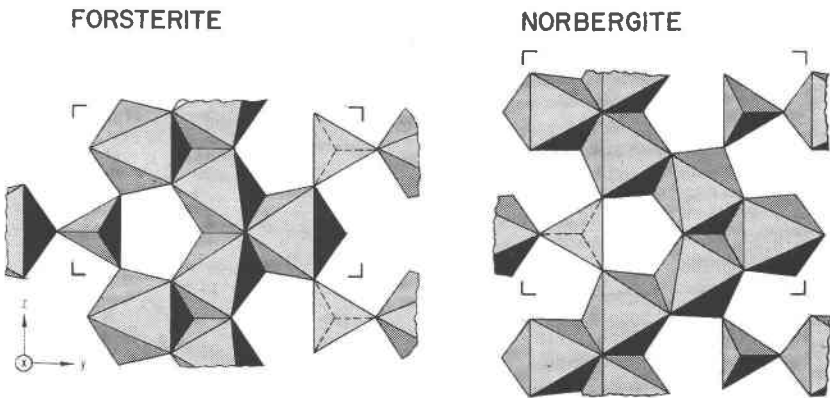


FIG. 1. The chains of edge-sharing Mg-octahedra in forsterite and norbergite, cross-linked by Si-tetrahedra. Unit cells are outlined. Compare with Figs. 1 and 3, Ribbe *et al.* (1968).

(1968) emphasized the structural similarity of norbergite and forsterite, pointing out that the replacement of four O by four F in the close-packed array of forsterite is balanced by the replacement of one tetrahedrally coordinated Si by a tetrahedral void, according to the general formula $Mg_{2x}Si_{x-1}O_{4x-4}(F)_4$ where $x=3$ for norbergite. This results in zigzag chains of edge-sharing Mg-octahedra alternating with chains of unoccupied octahedra running parallel to z and lying in the close-packed plane (100). Figure 1 compares the chains in forsterite and norbergite and shows the lateral linkages of the Mg-containing octahedra by Si-tetrahedra. Note that there are four octahedra in a period of the zigzag chain in forsterite, whereas there are six in norbergite. The Mg-octahedra in forsterite and norbergite only share edges; therefore, the Mg-octahedra in adjacent close-packed layers are related by b glides parallel to (100) at $\pm 1/4$ along x .

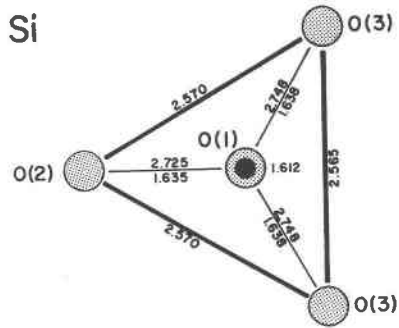


FIG. 2. The interatomic distances associated with the Si-tetrahedron. The heavy lines are edges shared with Mg-octahedra.

CATION COORDINATION

Tetrahedron. The SiO_4 group is a slightly distorted tetrahedron with C_s symmetry (Fig. 2). The O-Si-O angles opposite the edges shared with Mg-octahedra average 103.3° while those opposite unshared edges average 115.0° (Table 4). The shared edges average 2.568 \AA and are not significantly different; the unshared edges average 2.740 \AA . The Si-O bond lengths opposite shared edges are significantly longer ($1.635, 1.638 \text{ \AA}$)

INTERATOMIC DISTANCES (\AA)

Fo	No	Edges:	
3.134	3.138	— O-O	} Unshared Octahedral
	2.991	— F-O	
	2.915	— F-F	
2.857	2.826	— O-O	} Shared Octahedral
2.752	2.740	— O-O Unshared Tetrahedral	
	2.689	— F-O	
2.566	2.568	— O-O Shared Tetrahedral	
2.119	2.124	— Mg-O	} Octahedral Bond Length
	2.012	— Mg-F	
1.634	1.631	— Si-O Tetrahedral Bond Length	

FIG. 3. Comparison of the important interatomic distances in forsterite (Fo, Birle *et al.*, 1968) and norbergite (No, this paper) ordered on the basis of relative magnitudes. The values listed here replace the table in Gibbs and Ribbe (1968)

than that (1.612 Å) opposite the unshared edges. The mean Si-O bond of 1.631 Å is shorter than the 1.64 Å predicted by Shannon and Prewitt (private communication) and the 1.635 Å bond length predicted by Gibbs and Brown (1968) for Si bonded to a four-coordinated oxygen. A comparison of the important polyhedral interatomic distances for forsterite and norbergite are given in Fig. 3.

M(2) octahedron. The Mg with site symmetry C_2 is called M(2) by analogy with the M(2) site in forsterite (Birlé *et al.*, 1968). This is Mg_B of Taylor and West (1929). The M(2) octahedra in forsterite and norbergite are similar in every respect, except that in norbergite there are two F and

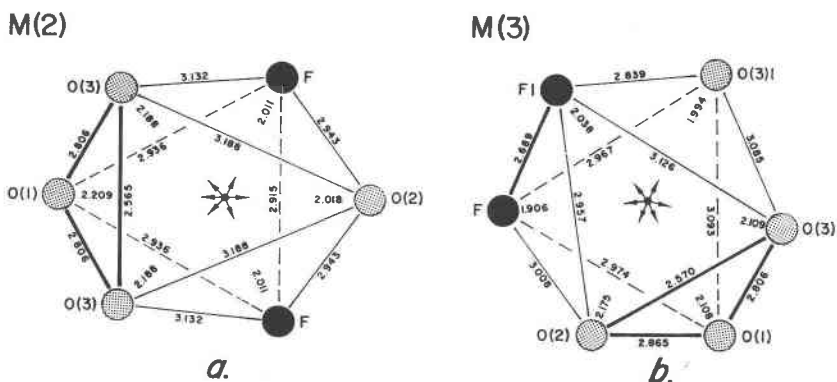


FIG. 4. The interatomic distances associated with (a) the M(2) octahedron and (b) the M(3) octahedron. The dark circles are fluorine, the light, oxygen. Heavy lines represent shared edges. The arrows indicate directions of Mg-O, F bonds.

four O anions instead of six O. As in forsterite two edges of an octahedral face (heavy lines in Fig. 4a) are shared with Mg-octahedra and one with the Si-tetrahedron. In norbergite the Mg is displaced ~ 0.1 Å from the geometric center of the octahedron away from this face toward the F anions, whereas in forsterite the displacement is less (~ 0.06 Å) because the Mg is coordinated only by larger O anions. In spite of the fact that the mean Mg-O bond length in M(2) in norbergite is larger than the corresponding mean Mg-O bond length in forsterite, the M(2) octahedron is slightly smaller (Mg-O, F = 2.104 Å) than it is in forsterite (Mg-O = 2.135 Å).

M(3) octahedron. The Mg with site symmetry C_1 (Mg_A of Taylor and West) is called M(3) in norbergite because this octahedron has four shared edges and is not equivalent to the M(1) of forsterite which has six

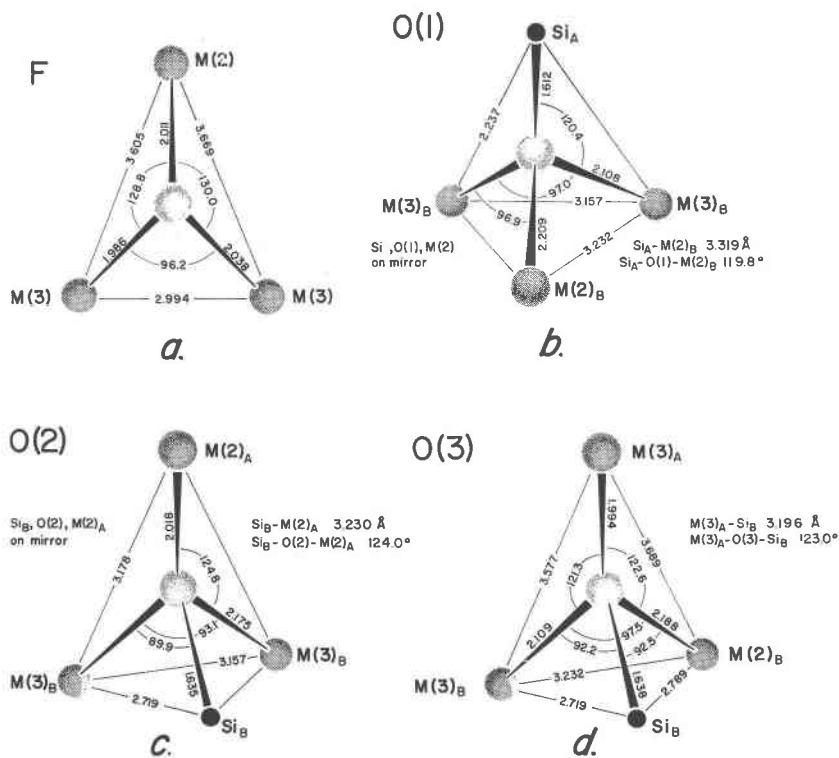


FIG. 5. The coordination, interatomic distances and angles for (a) fluorine, (b) oxygen O(1), (c) oxygen O(2) and (d) oxygen O(3). Dark circles are Mg, smaller black circles are Si. Subscript A indicates an apical atom, subscript B, a basal atom (see text). Angles and distances which could not be conveniently labelled are noted. Fig. 6a is a composite of b, c and d.

shared edges. However the M(1) type of octahedron does occur in chondrodite, humite and clinohumite, all of which contain M(2) and M(3) octahedra as well. The M(3) octahedron (Fig. 5b) shares an F-F edge and an O-O edge with other M(3) octahedra, one O-O edge with an M(2) octahedron, and one with the Si tetrahedron. The mean Mg-O,F bond length for the M(3) octahedron (2.055 Å) is smaller than M(2) in both norbergite and forsterite and is also smaller than M(1) in forsterite (2.103 Å) which has two more shared edges.¹ As expected this can be explained by the fact that four-coordinated O ($r = 1.38$ Å) is larger than three-co-

¹ It is of interest that the isotropic temperature factors for Mg in the larger M(2) site in both forsterite and norbergite are slightly greater than those calculated for the smaller M(1) and M(3) sites.

ordinated F ($r=1.30 \text{ \AA}$) (radii from Shannon and Prewitt, pers. commun.). The differences between the unshared octahedral O-O and F-F distances and the Mg-O and Mg-F bond lengths (Fig. 3) indicate that the O radius in norbergite is in effect 0.11 \AA larger than the F radius. This is consistent with the observation of Ribbe *et al.* (1968) that the normalized volume V' of forsterite is $\sim 2.1 \text{ \AA}^3$ larger than that of norbergite. A similar study of bond lengths involving two-coordinated F and three-coordinated O in topaz (Ribbe and Gibbs, in preparation) show O to be $\sim 0.12 \text{ \AA}$ larger in radius than F.

ANION COORDINATION

Fluorine. Fluorine is nearly coplanar with the three Mg cations to which it is bonded (Fig. 5a). In an ideal close-packed structure the M(2)-F-M(3) and the M(3)-F-M(3) angles are 131.8° and 90° , respectively. In norbergite the M(2)-F-M(3) angles are $2\text{--}3^\circ$ less than the ideal value; however, the M(3)-F-M(3) angle is 6° wider than the ideal, because the M(3) cations are repelled across an edge shared between their respective octahedra.

The isotropic temperature factor for the three-coordinated F ($B=0.74 \text{ \AA}^2$) is about twice as large as those calculated for the four-coordinated oxygens (Table 3). Although the difference in cation coordination accounts for part of the difference in temperature factor, the fact that the hcp array of anions is predominantly O (O:F = 2:1) and that F is $\sim 0.11 \text{ \AA}$ smaller than O accounts for the remainder of the difference.

Oxygen. Each oxygen in norbergite is coordinated by one Si, one M(2) and two M(3) cations (Fig. 5b, c, d). The angles that the metal cations subtend at each oxygen are remarkably similar although the "tetrahedral" distribution of Mg and Si around O(1) differs from that around O(2) or O(3). In each of these tetrahedral arrays of cations around O, there is one unique cation which subtends angles of $120\text{--}125^\circ$ at O with the three remaining cations. For convenience, this cation is called the apical cation (subscript A) and is oriented uppermost in Figure 5b, c, d. The remaining cations are called basal cations (subscript B) because they occur at the base of the tetrahedral array. The angle that these basal cations subtend at O is between $90\text{--}97^\circ$. The angles at O are listed in Table 5 together with the angles calculated for an ideal hcp array and the bond-angle strain (observed minus ideal).

The cation coordination of O(1) is different from O(2) and O(3) in that Si is at the apex and makes an angle of $\sim 120^\circ$ to the M(2) and M(3) cations at the oxygen. When Si is one of the basal cations, the angles to basal M cations at O(2) and O(3) range between 90° and 93° (ideally

TABLE 5. OBSERVED CATION-OXYGEN-CATION ANGLES FOR NORBERGITE COMPARED WITH THE ANGLES CALCULATED FOR AN IDEAL HEXAGONAL CLOSE-PACKED STRUCTURE. BOND-ANGLE STRAIN EQUALS OBSERVED MINUS IDEAL

	Observed	Ideal	Strain
Si _A -O(1)-M(2) _B	119.8	125.3	- 5.5
Si _A M(3) _B	120.4	125.3	- 4.9
M(2) _B M(3) _B	96.9	90.0	+ 6.9 ^b
M(3) _B M(3) _B	97.0	90.0	+ 7.0 ^b
mean	108.6	107.6	
M(2) _A -O(2)-Si _B	124.0	125.3	- 1.3
M(2) _A M(3) _B	124.8	131.8	- 7.0
M(3) _B M(3) _B	93.1	90.0	+ 3.1 ^b
M(3) _B Si _B	89.9	79.5	+10.4 ^a
mean	107.8	106.3	
M(3) _A -O(3)-Si _B	123.0	125.3	- 2.3
M(3) _A M(2) _B	122.6	131.8	- 9.2
M(3) _A M(3) _B	121.3	131.8	-10.5
M(3) _B M(2) _B	97.5	90.0	+ 7.5 ^b
M(3) _B Si _B	92.2	79.5	+12.7 ^a
M(2) _B Si _B	92.5	79.5	+13.0 ^a
mean	107.4	106.3	

^a Cations situated across an edge shared by an octahedron and a tetrahedron.

^b Cations situated across an edge shared by two octahedra.

79.5°). Bond-angle strains at both the oxygens and the cations are labeled in Figure 6 which is a composite of Figures 5b, c, d. From Figure 6 it can be shown that all bond-angle strains in norbergite can be explained by cation-cation repulsion across shared polyhedral edges. O(1)-O(2) and O(1)-O(3) are edges shared between Mg-octahedra; O(2)-O(3) and O(3)-O(3) are edges shared between a Mg-octahedron and a Si-tetrahedron (bold lines in Figs. 6b and 6c). Figs. 6b and 6c show, as expected from electrostatic considerations, that the bond-angle strains at the basal cations are negative and those at the anions are positive. When Mg_B-octahedra share edges (Fig. 6b), the strains at both Mg_B cations are very similar; but when a Mg_B-octahedron shares an edge with a Si_B-tetrahedron (Fig. 6c), the strains at Mg_B are 2-3 times greater. The strains at the highly charged Si_B, however, are considerably less than those at Mg_B. The relationships depicted in Fig. 6 are plotted in Fig. 7a. They show that the bond-angle strains at Mg_B vary regularly with the strains at O

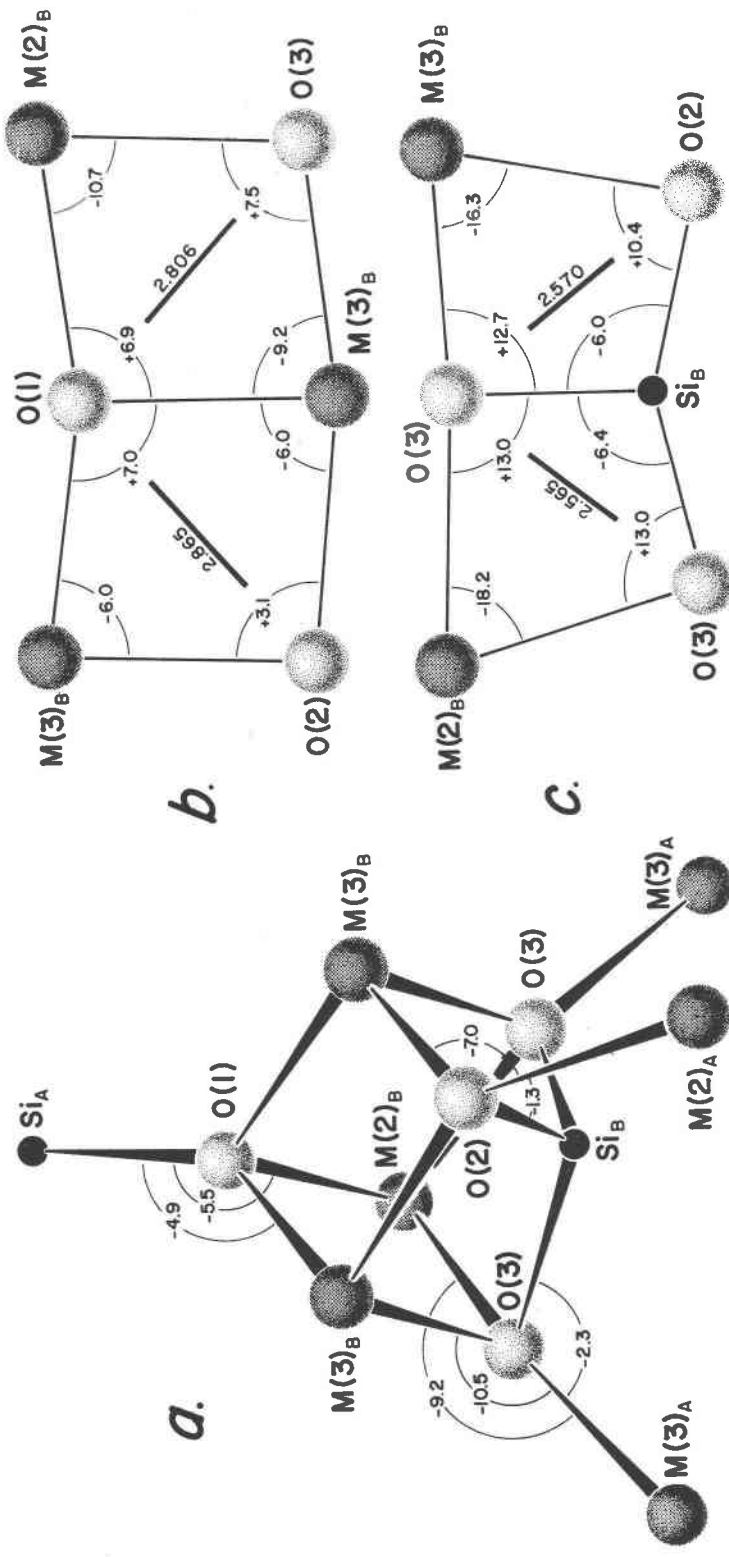


FIG. 6. (a) A composite of Figs. 5b, c and d showing apical bond-angle strains. (b and c) Drawings of the faces of the distorted cube made up of oxygens and basal cations in Fig. 6a. The heavy lines denote shared edges; their magnitudes (in Å) are given. The values (in degrees) given at the vertices are basal bond-angle strains.

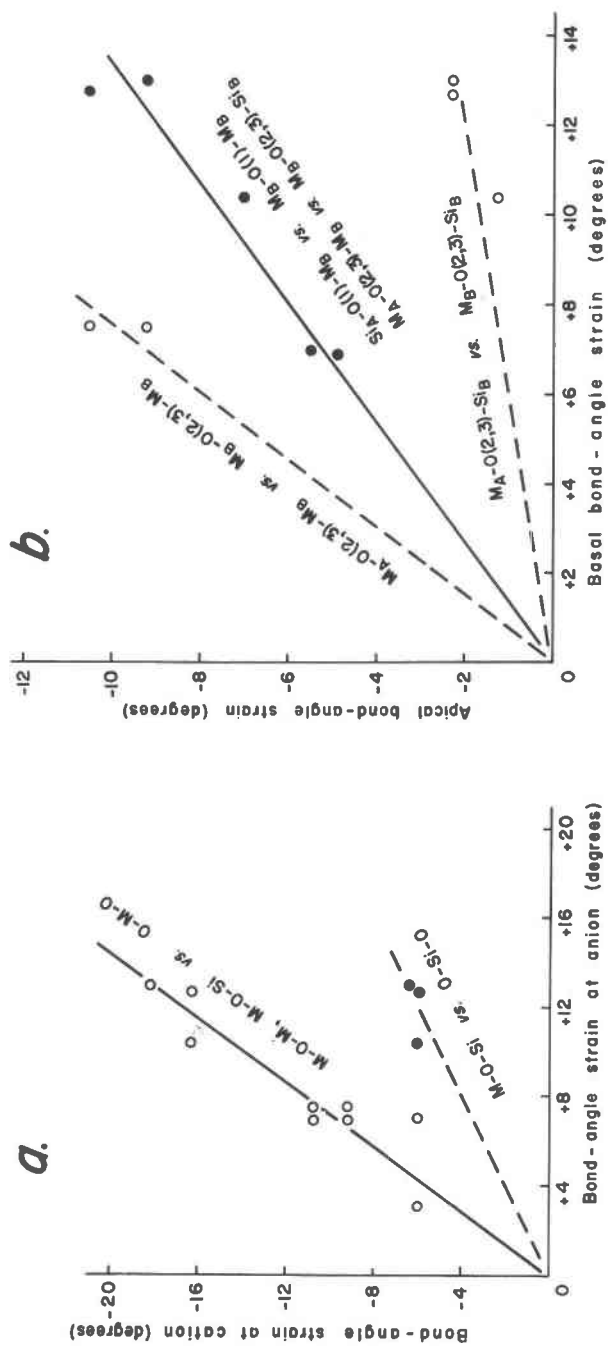


FIG. 7. (a) Bond-angle strains at the anions plotted against strains at the cations. (b) Basal vs. apical bond-angle strains at the oxygens.

and that the strains at Si_B are about one-third as great as those as Mg_B .

Also of interest are the relationships between the basal and the apical bond-angle strains at O(1), O(2) and O(3) (see Fig. 7b). The strains at O(2) and O(3) where Si is a basal cation (cf. Figs. 5c, d) are dominated by Si-Mg repulsion across the shared edges; this produces large positive strains in the basal angles $\text{M}_B\text{-O}(2, 3)\text{-Si}_B$ but only slight negative strains in the apical angles $\text{M}_A\text{-O}(2, 3)\text{-Si}_B$ (lower curve, Fig. 7b). The Si-Mg repulsion also induces positive strains in the $\text{M}_B\text{-O}(2, 3)\text{-M}_B$ angles and compensating negative strains in the $\text{M}_B\text{-O}(2, 3)\text{-M}_B$ angles. The tetrahedral array of cations around O(1) is unique. Here Si is the apical cation and three M cations are at the base. A second Si ion lies directly below the basal M_B cations of the array (Fig. 6a) which repels these three M_B cations equally toward Si_A . Consequently basal bond angle strains of $+6.9$ and 7.0° result which are compensated by strains in the apical angles of -4.9 and -5.5° . It should also be pointed out that M cations lie directly opposite the bases of the tetrahedral arrays around O(2) and O(3). However, because the bond angle strains $\text{M}_A\text{-O}(2, 3)\text{-Si}_B$ are small (-1.3 to -2.3°) it appears that the repulsive forces between these M cations and those at the bases of the tetrahedral arrays are second order in magnitude.

In conclusion it is apparent that the distortions from an ideal hexagonal close-packed model for norbergite can be explained qualitatively in terms of cation-cation repulsion across shared polyhedral edges. Further studies of this phenomenon are being undertaken on the other humite minerals and on the olivine minerals in which the effects of cations substituting for Mg will be examined and related to the Si-O bond.

ACKNOWLEDGEMENTS

We are grateful to Mr. K. Robinson of V.P.I. for measuring refractive indices and density. Prof. P. T. Chang, now at Grambling College, collected the intensity data. This work was supported by National Science Foundation Grant No. GA-1133. Profs. F. D. Bloss and P. B. Moore criticized the manuscript.

REFERENCES

- BIRLE, J. D., G. V. GIBBS, P. B. MOORE, AND J. V. SMITH (1968) Crystal structures of natural olivines. *Amer. Mineral.*, **53**, 807-824.
- BRAGG, W. L., AND G. B. BROWN (1926) Die Struktur des Olivins. *Z. Kristallogr.*, **63**, 538.
- , AND J. WEST (1927) The structure of certain silicates. *Proc. Roy. Soc. (London)*, **114**, 450-473.
- , AND G. F. CLARINGBULL (1965) *Crystal Structures of Minerals*. Cornell Univ. Press. Ithaca, N. Y., p. 175.
- BURNHAM, C. W. (1962) Lattice constant refinement. *Carnegie Inst. Wash. Year Bk.* **61**, 132-135.
- BUSING, W. R., K. O. MARTIN, AND H. A. LEVY (1962) ORFLS, a Fortran crystallographic

- least-squares program. Oak Ridge National Lab. [U.S. Clearinghouse Fed. Sci. Tech. Info.] Doc. ORNL-TM-305.
- (1964) ORFFE, a Fortran crystallographic function and error program. Oak Ridge National Lab. [U.S. Clearinghouse Fed. Sci. Tech. Info.] Doc. ORNL-TM-306.
- GEIJER, P. (1926) Norbergite and fluoborite, two new minerals from the Norberg mining district. *Geol. För. Förh. Stockholm*, **48**, 84–89.
- GIBBS, G. V., AND G. E. BROWN (1968) Oxygen coordination and the Si-O bond. (abstr.). *Geol. Soc. Amer. SE Sec. Meet.*, Durham, N. C., 89.
- , AND P. H. RIBBE (1968) The crystal structures of the humite minerals. I. Norbergite. (abstr.). *Int. Mineral. Ass.*, Prague, 75–76.
- IBERS, J. A. (1956) Estimates of the standard deviations of the observed structure factors and of the electron density from intensity data. *Acta Crystallogr.* **9**, 652–654.
- JONES, N. W., P. H. RIBBE AND G. V. GIBBS (1969) Crystal chemistry of the humite minerals. *Amer. Mineral.*, **54**, 391–411.
- PENFIELD, S. L. AND W. T. H. HOWE (1894) On the chemical composition of chondrodite, humite and clinohumite. *Amer. J. Sci., Ser. 3*, **47**, 188–206.
- RIBBE, P. H., G. V. GIBBS, AND N. W. JONES (1968) Cation and anion substitutions in the humite minerals. *Mineral. Mag.*, **37**, 966–975.
- TAYLOR, W. H. AND J. WEST (1928) The crystal structure of the chondrodite series. *Proc. Roy. Soc. (London)*, **117**, 517–532.
- (1929) The structure of norbergite. *Z. Kristallogr.* **70**, 461–474.
- VAN VALKENBURG, A. (1961) Synthesis of the humites $n\text{Mg}_2\text{SiO}_4 \cdot \text{Mg}(\text{F},\text{OH})_2$. *J. Res. Nat. Bur. Stand.*, **65A**, 415–428.
- WASER, J. (1955) The anisotropic temperature factor in triclinic coordinates. *Acta Crystallogr.* **8**, 732.

Manuscript received September 19, 1968; accepted for publication December 16, 1968.